DYNAMIC ANALYSIS OF A THREE-ROTOR FLEXIBLE COUPLING WITH ANGULAR MISALIGNMENT

M. Akhondizadeh. Korrani*

Mechanical Engineering Department of Shahid Bahonar University of Kerman, Kerman-Iran
mehdi2089@yahoo.com

M. Fooladi. Mahani

Mechanical Engineering Department of Shahid Bahonar University of Kerman, Kerman-Iran
fooladi@mail.uk.ac.ir

*Corresponding Author

Abstract   In this paper, the dynamic response of a three-rotor flexible coupling to the angular misalignment has been studied. The coupling is a power transmission agent between the motor and gearbox, in the power transmission system of SAG Mill (semi autogenously mill) in the Gol-e-Gohar iron ore complex in Sirjan, Iran. Degrees of freedom of the system are the model's lateral deflections and the rigid-body linear motions. The equations of motion are obtained by using the Lagrange equations through successive partial differentiation of the kinetic and potential energies. In the dynamic model, the middle rotor is considered as an eccentric flexible Jeffcott rotor. The gearbox input shaft is considered to be angularly misaligned with respect to the motor shaft. Diagrams of the amplitudes versus the frequency ratio reveal the system dynamic response to the angular misalignment.

Keywords   Rotor dynamic, Flexible coupling, Misalignment, Vibration,

<div dir="rtl">

چکیده   در کار حاضر، پاسخ دینامیکی یک کوپلینگ انعطاف‌پذیر شامل سه روتور با ناهم‌راستایی زاویه‌ای مورد بررسی قرار گرفته است. این کوپلینگ، واسط انتقال قدرت بین موتور و گیربکس در سیستم انتقال قدرت آسیای نیمه خودشکن معدن سنگ آهن گل گهر سیرجان در ایران است. درجات آزادی سیستم، انعطاف جانبی در سیستم و حرکات خطی جسم صلب هستند. معادلات حرکت سیستم با روش دینامیک لاگرانژی و با مشتق گیری پیاپی از انرژی‌های جنبشی و پتانسیل استخراج می‌شوند. در مدل دینامیکی، روتور میانی، یک روتور انعطاف‌پذیر مدل جفکات دارای خروج از مرکز، در نظر گرفته شده است. ناهم‌راستایی زاویه‌ای برای محور ورودی گیربکس نسبت به محور خروجی موتور درنظر گرفته می‌شود. نمودارهای دامنه بر حسب فرکانس نسبی، پاسخ سیستم به ناهم‌راستایی زاویه‌ای را آشکار می‌سازد.

</div>

1. INTRODUCTION

Couplings are widely used in industry to transmit the power from the driver to the driven rotors. Generally, there are two types of connections in couplings: rigid and flexible. Rigid couplings have low deflections; however, they insert additional force and moments on the system equipments such as motor, bearings and gearbox. Flexible couplings are used to eliminate the additional force and moments; however, their position changes may be resulted in high level vibrations that can damage the system and lead to shutdown.

Misalignment of the connected rotors is one of the most common defects that may be encountered. It may cause undesired vibrations. Many factors affect the vibration behavior of a misaligned system. Therefore the phenomenon must be well understood so that it can be detected and adjusted at the initial stages of its appearance.

There are a lot of discussions in industry regarding the interpretation of the vibration signals introduced due to misalignment, but there is not enough academic research to explain the phenomenon in a simple way.

Al-Hussain [1] studied the dynamic behavior of a two-rotor rigid coupling model exposed to parallel

misalignment, to aid turbo machinery diagnostic engineers in understanding the dynamic response of a misaligned system. He proposed future works such as angular misalignment and axial motions. Lorenzen et al. [2] compared the critical speeds of a high-speed high-power compressor train that alternatively equipped with the solid couplings, flexible-disc and gear-type couplings. They showed that the solid couplings can cause the rotor to be more stable. Sekhar and Prabhu [3] explained the effect of the coupling misalignment on the turbo machinery vibrations. They showed that the location of the coupling has a strong influence on the level of vibrations. A theoretical model of a complete system of the motor-flexible coupling rotor was presented by Xu and Marangoni [4]. They assumed that the flexible coupling behaves exactly like a universal joint to take the misalignment effect into account. Prabhu [5] experimentally investigated the effect of misalignment on the cylindrical and three-lobe journal bearings. He showed that an increase in the angular misalignment caused change in the second harmonic of the vibration response. Simon [6] predicted the behavior of a large imbalanced turbo machine, imposed by the misalignment. He computed numerically the vibration, excited by the coupling, using the assumed values for the coupling reaction force and moments.

Diagnostic engineers of the Gol-e-Gohar industry aimed to develop a VCM (vibration condition monitoring) process on the power transmission system of the SAG Mill. Misalignment is one of the common system defects, so its dynamic effects must be good understood. In the present work the system dynamic response to the angular misalignment has been investigated.

2. GEOMETRY DESCRIPTION

The system that transmits power between a 3Mwatt-motor and the gearbox of a SAG Mill is studied here. It is composed of output motor-side shaft, flexible coupling and gearbox input shaft. The flexible coupling is illustrated in Figure 1. The motor shaft and gearbox input shaft are located inside the hubs 1 and 3 respectively. The geometrical system properties are shown in Table 1.

TABLE 1. Geometrical system properties

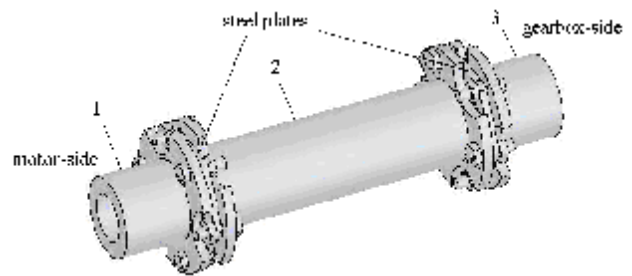| Shaft	Length (mm)	Diameter (mm)	Length to diameter ratios
Motor shaft	320	220	1.45
Flexible shaft	1260	D_o =368, D_i =324	3.42
Gearbox shaft	240	220	1.1

Figure 1. Coupling with steel plates as the flexible elements

3. DYNAMIC MODEL

The system model with angular misalignment is illustrated in Figure 2. The angular misalignment of the gearbox input shaft relative to the motor output shaft is taken as a pure rotation around the *y* axis as shown in Figure 2. In this figure, γ is the angular misalignment magnitude and α is the orientation change of rotor 2 due to the misalignment.
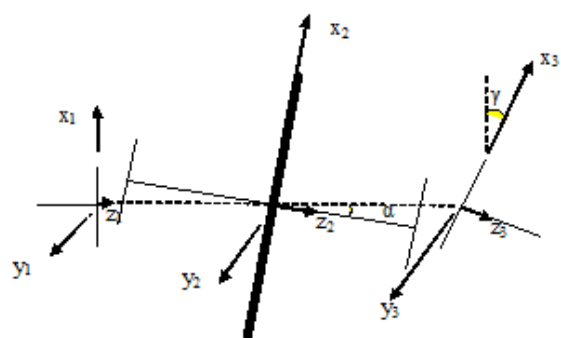

Figure 2. Model of the misaligned system

Rotor 2 is considered as an imbalanced flexible Jeffcott rotor. Figure 3 shows the position of the area and mass centers of rotor 2 at an instant of the

motion, and the point o corresponds to the end position of rotor 2 at this instant. The length-diameter ratios of rotors 1 and 3 are such that they can be considered as rigid cylinders.

4. KINETIC AND POTENTIAL ENERGIES

The Lagrange energy method is used to obtain the equations of motion. The generalized coordinates for the 13 degrees of freedom of the system are:
$$q = \{x_1, y_1, z_1, \beta_1, x_o, y_o, z_o, x_{r2}, y_{r2}, x_3, y_3, z_3, \beta_3\} \quad (1)$$
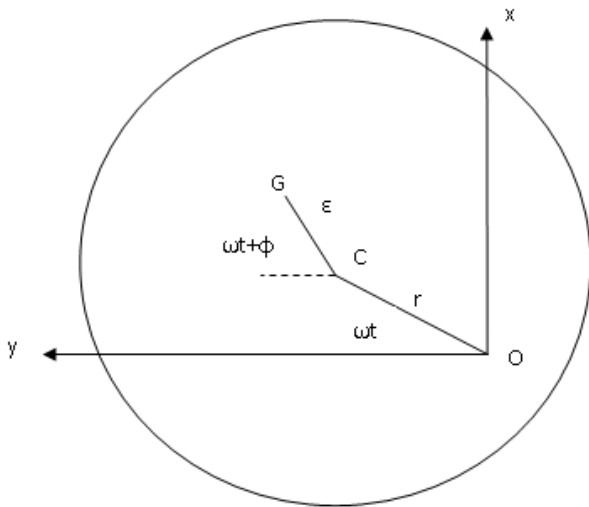

Figure 3. Position of rotor 2 at an instant of the motion

Independent coordinates, r and $\beta_2 = \omega t$, specify the position of center mass of rotor 2 with respect to its ends but, in the present study, they have been replaced by the coordinates x_{r2} and y_{r2} respectively. So, the position of the center of mass of rotor 2 with respect to its static state is specified as follows:

$$x_2 = x_o + x_{r2} \quad (2)$$

$$y_2 = y_o + y_{r2} \quad (3)$$

$$x_{r2} = r \sin\omega t + \varepsilon \sin(\omega t + \varphi) \quad (4)$$

$$y_{r2} = r \cos\omega t + \varepsilon \cos(\omega t + \varphi) \quad (5)$$

The rotations of rotor 2 around the x and y axes have been ignored. Therefore:

$$z_2 = z_o \quad (6)$$

the system kinetic energy is:

$$T = T_1 + T_2 + T_3 \quad (7)$$

$$T = \frac{1}{2}m_1(\dot{x}_1^2 + \dot{y}_1^2 + \dot{z}_1^2) + \frac{1}{2}\bar{I}_1\dot{\beta}_1^2$$
$$+ \frac{1}{2}m_2[(\dot{x}_o + \dot{x}_{r2})^2 + (\dot{y}_o + \dot{y}_{r2})^2 + \dot{z}_o^2]$$
$$+ \frac{1}{2}\bar{I}_2\dot{\beta}_2^2 + \frac{1}{2}m_3(\dot{x}_3^2 + \dot{y}_3^2 + \dot{z}_3^2) + \frac{1}{2}\bar{I}_3\dot{\beta}_3^2 \quad (8)$$

and the potential energy is:
$$U = U_{bm} + U_{bg} + U_2 + U_{c1} + U_{c2} \quad (9)$$

It is assumed that the bearings are linearly flexible and their potential energy is as follows[1]:

$$U_{bm} = \frac{1}{2}k_{bmx}x_1^2 + \frac{1}{2}k_{bmy}y_1^2 + \frac{1}{2}k_{bmz}z_1^2 \quad (10)$$

$$U_{bg} = \frac{1}{2}k_{bgx}x_3^2 + \frac{1}{2}k_{bgy}y_3^2 + \frac{1}{2}k_{bgz}z_3^2 \quad (11)$$

The potential energy of the flexible connections is due to the relative motion of the ends of rotor 2 with respect to the rotors 1 and 3 [7]. The end displacements of rotor 2 in direction of rotors 1 and 3 can be written by using unit vectors as:

$$\mathbf{r}_{c21} = (x_o \cos\alpha - z_o \sin\alpha)\mathbf{i}_1 + y_o\mathbf{j}_1 + (x_o \sin\alpha + z_o \cos\alpha)\mathbf{k}_1 \quad (12)$$

$$\mathbf{r}_{c23} = [x_o \cos(\gamma - \alpha) - z_o \sin(\gamma - \alpha)]\mathbf{i}_3 + y_o\mathbf{j}_3 + [x_o \sin(\gamma - \alpha) + z_o \cos(\gamma - \alpha)]\mathbf{k}_3 \quad (13)$$

then, the potential energy of the connection is:

$$U_{c21} = \frac{1}{2}k_{cx}\{x_o \cos a - z_o \sin a - x_1\}^2$$
$$+ \frac{1}{2}(y_o - y_1)^2 + \frac{1}{2}k_{cz}\{x_o \sin a + z_o \cos a - z_1\}^2 \quad (14)$$

$$U_{c23} = \frac{1}{2}k_{cx}\{x_o \cos(g - a)$$
$$- z_o \sin(g - a) - x_3\}^2$$
$$+ \frac{1}{2}k_{cy}(y_o - y_3)^2 + \frac{1}{2}\{x_o \sin(g - a)$$
$$+ z_o \cos(g - a) - z_3\}^2 \quad (15)$$

Bending potential energy of rotor 2 is:
$$U_2 = \frac{1}{2}k_2r^2 = \frac{1}{2}k_2\{[x_{r2} - e \sin(wt + j)]^2$$
$$+ [y_{r2} - e \cos(wt + j)]^2\} \quad (16)$$

Total potential energy of the system is the sum of all potential energies, is:

$$U = \frac{1}{2} k_{bmx} x_1^2 + \frac{1}{2} k_{bmy} y_1^2 + \frac{1}{2} k_{bmz} z_1^2$$
$$+ \frac{1}{2} k_{bgx} x_3^2 + \frac{1}{2} k_{bgy} y_3^2 + \frac{1}{2} k_{bgz} z_3^2$$
$$+ \frac{1}{2} k_{cx} \{ x_o \cos a - z_o \sin a - x_1 \}^2$$
$$+ \frac{1}{2} k_{cy} (y_o - y_1)^2 + \frac{1}{2} k_{cz} \{ x_o \sin a +$$
$$z_o \cos a - z_1 \}^2 + \frac{1}{2} k_{cx} \{ x_o \cos(g - a)$$
$$- z_o \sin(g - a) - x_3 \}^2 + \frac{1}{2} k_{cy} (y_o - y_3)^2$$
$$+ \frac{1}{2} k_{cz} \{ x_o \sin(g - a) + z_o \cos(g - a)$$
$$- z_3 \}^2 + \frac{1}{2} k_2 \{ (x_{r2} - e \sin(wt + j))^2$$
$$+ (y_{r2} - e \cos(wt + j))^2 \} \tag{17}$$

5. EQUATIONS OF MOTION

Equation (18) (Lagrange's equation) is used to obtain the equations of motion.

$$\frac{d}{dt}(\frac{\partial T}{\partial \dot{q}_i}) + \frac{\partial U}{\partial q_i} - \frac{\partial T}{\partial q_i} = Q_i, \qquad i = 1, 2, 3, \ldots, n \tag{18}$$

where, n is the number of generalized coordinates and Q_i is the generalized force(or moment) in direction of q_i.

$$\frac{d}{dt}(\frac{\partial T}{\partial \dot{x}_1}) + \frac{\partial U}{\partial x_1} - \frac{\partial T}{\partial x_1} = Q_{x1}$$
$$\frac{d}{dt}(m_1 \dot{x}_1) + k_{bmx} x_1 - k_{cx} \{ x_o \cos a - z_o \sin a - x_1 \} = -C_{x1} \dot{x}_1 \tag{19}$$
$$m_1 \ddot{x}_1 + C_{x1} \dot{x}_1 + (k_{bmx} + k_{cx}) x_1 = k_{cx} (x_o \cos a - z_o \sin a)$$
$$m_1 \ddot{y}_1 + C_{y1} \dot{y}_1 + (k_{bmy} + k_{cy}) y_1 = k_{cy} y_o \tag{20}$$
$$m_1 \ddot{z}_1 + C_{z1} \dot{z}_1 + (k_{bzm} + k_{cz}) z_1 = \tag{21}$$
$$k_{cz} (x_o \sin a + z_o \cos a)$$
$$m_3 \ddot{x}_3 + C_{x3} \dot{x}_3 + (k_{bgx} + k_{cx}) x_3 = \tag{22}$$
$$k_{cx} [x_o \cos(g - a) - z_o \sin(g - a)]$$
$$m_3 \ddot{y}_3 + C_{y3} \dot{y}_3 + (k_{bgy} + k_{cy}) y_3 = k_{cy} y_o \tag{23}$$
$$m_3 \ddot{z}_3 + C_{z3} \dot{z}_3 + (k_{bgz} + k_{cz}) z_3 = $$
$$k_{cz} [x_o \sin(g - a) + z_o \cos(g - a)] \tag{24}$$

It can be inferred from Equations (19)-(24) that the dynamic of rotors 1 and 3 is highly dependent on the end movement of rotor 2.
Equations of motion of rotor 2 are:

$$\frac{d}{dt}(\frac{\partial T}{\partial \dot{x}_{r2}}) + \frac{\partial U}{\partial x_{r2}} - \frac{\partial T}{\partial x_{r2}} = Q_{xr2}$$
$$m_2 (\ddot{x}_{r2} + \ddot{x}_o) + k_2 [x_{r2} - e \sin(wt + j)] = 0 \tag{25}$$

Substituting x_{r2} from Equation (4) into Equation (25) leads to:

$$m_2 \ddot{x}_o = m_2 w^2 [r \sin wt + e \sin(wt + j)]$$
$$- k_2 r \sin wt \tag{26}$$

At the steady state, r and φ are independent of time and can be expressed as Equations (27). [10]

$$r(w) = \frac{e(\frac{w}{w_{n2}})^2}{\sqrt{(2x_2 \frac{w}{w_{n2}})^2 + (1 - (\frac{w}{w_{n2}})^2)^2}}$$
$$j(w) = \tan^{-1}[\frac{2x_2 \frac{w}{w_{n2}}}{1 - (\frac{w}{w_{n2}})^2}] \tag{27}$$

where

$$w_{n2} = \sqrt{\frac{k_2}{m_2}} \quad \text{and} \quad x_2 = \frac{C_2}{2\sqrt{k_2 m_2}} \tag{28}$$

are the bending natural frequency and damping ratio of rotor 2.
Therefore, the solution of Equation (26) can be given as:
$$x_o(t, w) = X_o(w) \cos(wt - q_{xo}) \tag{29}$$
where
$$X_o(w) = \sqrt{[r(\frac{w_{n2}}{w})^2 - r - e \cos j]^2 + e^2 \sin^2 j} \tag{30}$$
$$q_{xo}(w) = \tan^{-1}[\frac{r(\frac{w_{n2}}{w})^2 - r - e \cos j}{-e \sin j}]$$

The equation of motion of rotor 2 in direction of y is solved in the same way as that for direction of x, to obtain the end displacement, y_o, as a function of time and rotational frequency.
$$m_2 \ddot{y}_o = m_2 w^2 [r \cos wt + e \cos(wt + j)] - $$
$$k_2 r \cos wt \Rightarrow y_o(t, w) = Y_o(w) \cos(wt - q_{yo}) \tag{31}$$
where

$$Y_o(w) = \sqrt{[r(\frac{W_{n2}}{w})^2 - r - e\cos j]^2 + e^2 \sin^2 j}$$

$$q_{yo}(w) = \tan^{-1}[\frac{e\sin j}{r(\frac{W_{n2}}{w})^2 - r - e\cos j}]$$
(32)

6. SOLUTIONS

Substituting Equations (29) and (31) into Equations (19) to (24):

$$m_1 \ddot{y}_1 + C_{y1} \dot{y}_1 + (k_{bmy} + k_{cy})y_1 = \\ k_{cy}Y_o(w)\cos(wt - q_{yo})$$
(33)

It is assumed that:

$$y_1(t,w) = \text{Real}(Y_1 e^{iwt})$$
(34)

where $i = \sqrt{-1}$. Substituting $y_1(t,\omega)$ from Equation (34) into the Equation (33) leads to:

$$[-w^2 + i\frac{C_{y1}w}{m_1} + (\frac{k_{bmy} + k_{cy}}{m_1})]Y_1 = \frac{k_{cy}}{m_1}Y_o(w)e^{-iq_{y0}}$$
(35)

solution of Equation (35) for Y_1, gives:

$$Y_1(w) = \frac{\frac{k_{cy}}{k_{bmy}}Y_o(w)}{\sqrt{(2x_{y1}\frac{w}{w_{n1y}})^2 + [1 + \frac{k_{cy}}{k_{bmy}} - (\frac{w}{w_{n1y}})^2]^2}}e^{-i(q_{yo}+q_{y1})}$$
(36)

where

$$w_{n1y} = \sqrt{\frac{k_{bmy}}{m_1}}, \qquad x_{y1} = \frac{C_{y1}}{2\sqrt{k_{bmy}m_1}},$$

$$q_{y1} = \tan^{-1}[\frac{2x_{y1}\frac{w}{w_{n1}}}{1 + \frac{k_{cy}}{k_{bmy}} - (\frac{w}{w_{n1y}})^2}]$$
(37)

Therefore:

$$y_1(t,w) = \frac{\frac{k_{cy}}{k_{bmy}}Y_o(w)}{\sqrt{(2x_{y1}\frac{w}{w_{n1y}})^2 + [1 + \frac{k_{cy}}{k_{bmy}} - (\frac{w}{w_{n1y}})^2]^2}}\cos(wt - q_{yo} - q_{y1})$$
(38)

Equation (19), which is a couple equation of x_1, x_o and z_o, is solved to determine $x_1(t,\omega)$. A reasonable assumption that z_o is a harmonic function in phase with x_o, simplifies the solution of Equation (19).

$$z_o(t,w) = Z_o \cos(wt - q_{xo})$$
(39)

Substituting Equations (39) and (29) into Equation (19), leads to:

$$\ddot{x}_1 + \frac{C_{x1}}{m_1}\dot{x}_1 + (\frac{k_{bmx} + k_{cx}}{m_1})x_1 = \frac{k_{cx}}{m_1}[X_o(w)\cos a$$
$$- Z_o \sin a]\cos(wt - q_{xo})$$
(40)

A solution for the Equation (40) would be:

$$x_1(t,w) = \text{Real}(X_1(w)e^{iwt})$$
(41)

Substituting Equation (41) into Equation (40) leads to:

$$x_1(t,w) = \frac{\frac{k_{cx}}{k_{bmx}}[X_o(w)\cos a - Z_o \sin a]}{\sqrt{(2x_{x1}\frac{w}{w_{n1x}})^2 + [1 + \frac{k_{cx}}{k_{bmx}} - (\frac{w}{w_{n1x}})^2]^2}}\cos(wt - q_{xo} - q_{x1})$$
(42)

Where

$$x_{x1} = \frac{C_{x1}}{2\sqrt{k_{bmx}m_1}}, \qquad q_{x1} = \tan^{-1}[\frac{2x_{x1}\frac{w}{w_{n1x}}}{1 + \frac{k_{cx}}{k_{bmx}} - (\frac{w}{w_{n1x}})^2}],$$
(43)

$$W_{n1x} = \sqrt{\frac{k_{bmx}}{m_1}}$$

Solution of Equation (21) by the same method as Equation (19) leads to:

$$z_1(t,w) = \frac{\frac{k_{cz}}{k_{bmz}}[X_o(w)\sin a + Z_o \cos a]}{\sqrt{(2x_{z1}\frac{w}{w_{n1z}})^2 + [1 + \frac{k_{cz}}{k_{bmz}} - (\frac{w}{w_{n1z}})^2]^2}}\cos(wt - q_{xo} - q_{z1})$$
(44)

where

$$x_{z1} = \frac{C_{z1}}{2\sqrt{k_{bmz}m_1}}, \quad W_{n1z} = \sqrt{\frac{k_{bmz}}{m_1}}$$

$$q_{z1} = \tan^{-1}[\frac{2x_{z1}\frac{w}{w_{n1z}}}{1 + \frac{k_{cz}}{k_{bmz}} - (\frac{w}{w_{n1z}})^2}],$$
(45)

This research is carried out in a real system, so the real mechanical parameters which have been listed in Table 2 should be used for the numerical analysis.

TABLE 2. System mechanical parameters

k_{cx}	k_{cy}	k_{cz}
1.22 GN/m	1.22 GN/m	0.735GN/m
m_1	m_2	m_3
313 kg	313 kg	289 kg

Equation (46) is used to calculate the stiffness of roller bearings [8].

$$K_{eq} = 3 \times 10^5 N^{0.9} L^{0.8} P^{0.1} \cos^{1.9} \alpha_1 \, (lb/in) \quad (46)$$

Therefor the stiffness of the motor-side bearing would be:

$$k_{bm} = 3 \times 10^5 \times 19^{0.9} \times 1.97^{0.8} \times 1046.4^{0.1} = 146.4 \times 10^5$$
$$lb/in = 2.53 \, GN/m \quad (47)$$

Bending stiffness of rotor 2, as a beam, can be calculated as follow: [9]

$$k_2 = \frac{48 E I_2}{l_2^3} = 3.6 * 10^8 \, N/m \quad (48)$$

7. NUMERICAL RESULTS

To study the effect of rotational frequency on the dynamic response of the system, results of the case study where $Z_o/\varepsilon = 2$ and $\alpha = 7$ degrees were calculated. It should be noted that α is not the angular misalignment magnitude, and is the rotor 2 orientation change due to the misalignment. Dimensionless form of the amplitude function of rotor 1 in direction of z_1 is written as:

$$\frac{Z_1(w)}{e} = \frac{\frac{k_{cz}}{k_{bmz}}[\sin a \sqrt{[\frac{r}{e}(\frac{W_{n2}}{W_{n1z}})(\frac{W_{n1z}}{W})^2 - \frac{r}{e} - \cos j]^2 + \sin^2 j} + \frac{Z_o}{e}\cos a]}{\sqrt{(2x_{z1}\frac{W}{W_{n1z}})^2 + [1 + \frac{k_{cz}}{k_{bmz}} - (\frac{W}{W_{n1z}})^2]^2}} \quad (49)$$

In the Equation (49), r and φ depend on the rotational velocity, eccentricity value, damping ratio and bending stiffness of rotor 2. After substituting Equation (27) into Equation (49), the dimensionless amplitude Z_1/ε would be a function of the rotating frequency only. The dimensionless

amplitude of rotor 1 in x and y directions as the functions of rotational frequency can be obtained by the same procedure as that of z direction.
Variations of the dimensionless amplitudes versus the frequency ratio, for damping ratios of 0.05-1, have been illustrated in Figures 4 to 8.
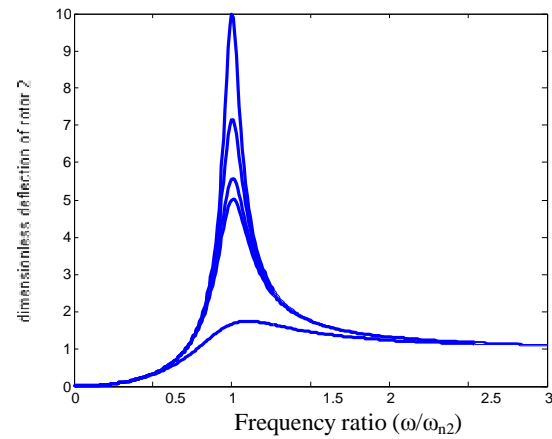

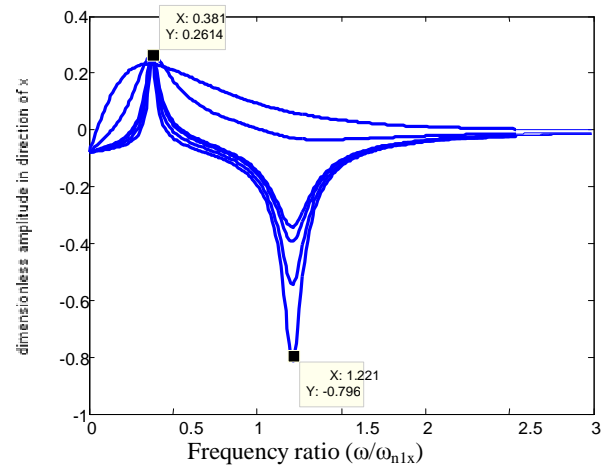**Figure 4**. Dimensionless amplitude of rotor 1 in z direction (Z_1/ε), versus the frequency ratio (ω/ω_{n1z})

Figure 5. Dimensionless amplitude of rotor 1 in x direction (X_1/ε), versus the frequency ratio (ω/ω_{n1x})
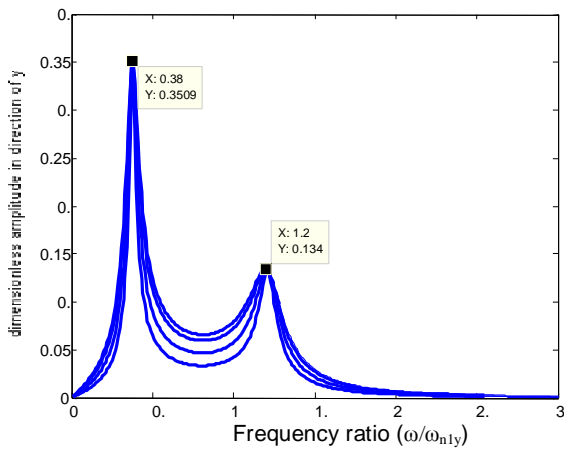
Figure 6. Dimensionless amplitude of rotor 1 in y direction (Y_1/ε), versus the frequency ratio (ω/ω_{n1y})
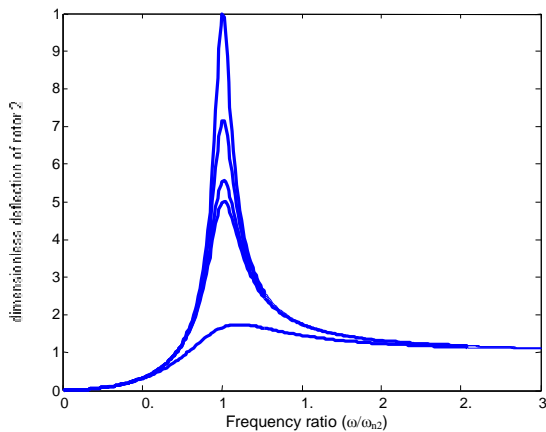
Figure 7. Dimensionless deflection of rotor 2 (r/ε), versus the frequency ratio (ω/ω_{n2})
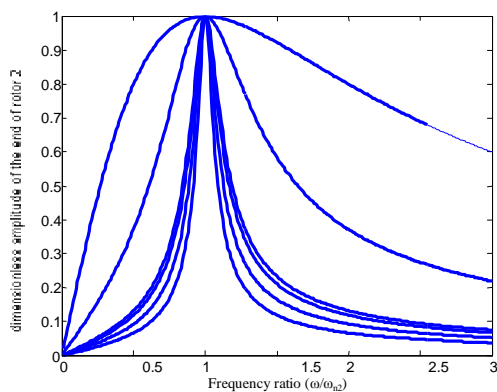
Figure 8. Dimensionless end movement of rotor 2 (X_o/ε), versus the frequency ratio (ω/ω_{n2})

Figures 4-6 show resonances on the frequency spectrums of rotor 1 that corresponds to the frequency ratios of 0.38 and 1.2 for the spectrums of x and y directions, and the frequency ratio of 1.32 for the spectrum of z direction. The resonance frequency ratios of the x and y directions are equal because:

$k_{cx}= k_{cy}$ and $k_{bmx}= k_{bmy}$.

As is shown in Figure 8, when $\omega/\omega_{n2}=1$ then $X_o/\varepsilon=1$ The reason is clear from the Equation (50).

$$\frac{X_o(w)}{e} = \frac{1}{\sqrt{\{(\frac{[1-(\frac{w}{w_{n2}})^2]}{\sqrt{(2x_2\frac{w}{w_{n2}})^2 + (1-(\frac{w}{w_{n2}})^2)^2}})-\cos j\}^2 + \sin^2 j}} \quad (50)$$

The first harmonic of Figures 5 and 6 is similar to that of Figure 8. This is because the first resonance arises from the excitation source harmonic, i.e., the rotor 2 harmonic. So, when the rotational frequency approaches the natural frequency of rotor 2, the resonance behavior of rotor 1 is similar to that of the end of rotor 2. This is not clear on the frequency spectrum of z direction in Figure(4), because the level of its second resonance is very high relative to the first one due to relatively high selected value for Z_o/ε. Variation of the dimensionless amplitude of rotor 1 in z direction versus the frequency ratio and Z_o/ε has been illustrated in Figure 9. It can be seen in this figure that for the small values of Z_o/ε, the frequency spectrum of z direction is the same as the spectrums of x and y directions.
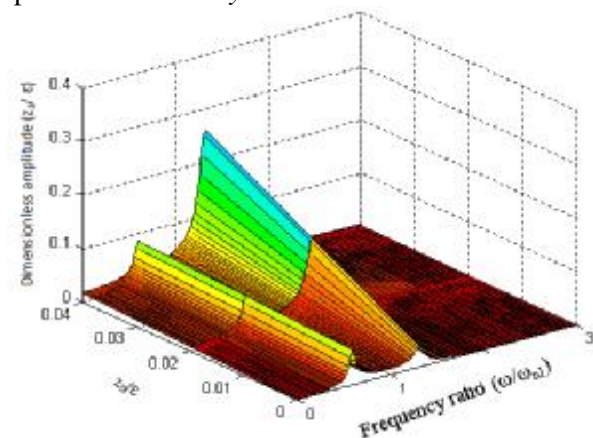

Figure 9. Dimensionless frequency spectrum of rotor 1 in z direction, versus Z_o/ε and frequency ratio

It can be seen in Figures 4 to 6 that the resonance frequency ratios do not correspond to the "1x" or "2x" of the rotational frequency, response characteristics commonly observed in the field of misaligned rotating shaft systems. The first harmonic at the spectrums corresponds to the case that $\omega = \omega_{n2}$, however, it corresponds to the case that $\omega/\omega_{n1x} = \omega/\omega_{n1y} = 0.38$. The second harmonic also corresponds to the case:

$$1 + \frac{k_{cz}}{k_{bmz}} - (\frac{W}{W_{n1z}})^2 = 0 \qquad (51)$$

So, the harmonic of the frequency spectrums of rotor 1 do not correspond to the frequency ratios of 1.

8. VARIATION OF THE MISALIGNMENT ANGLE

In this section, the effect of the angular misalignment on the system dynamic is investigated by providing the three dimensional amplitude diagrams versus the orientation change of rotor 2 (α) and the frequency ratio. In these diagrams, the large variation interval of α, [0, 0.4]... has been used so that its effects can be clearly shown. Otherwise, the value of α=0.4 radian is practically a very high angular misalignment value.
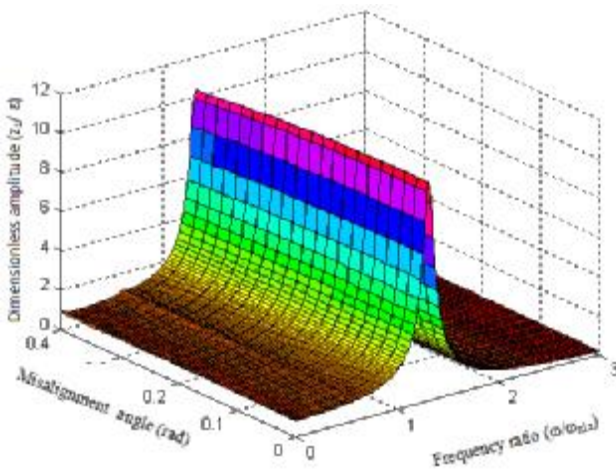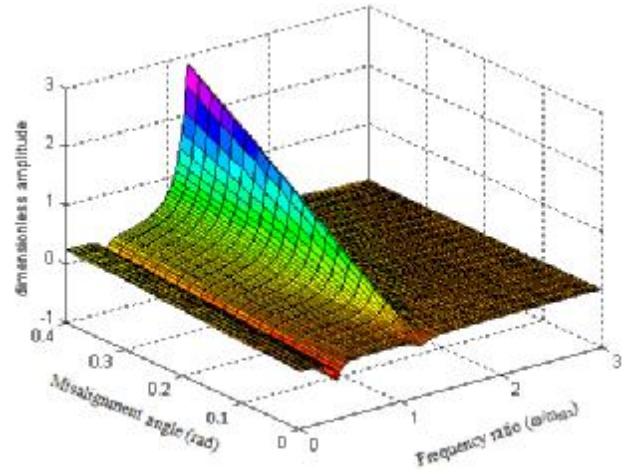

Figure 11. Three dimensional diagram of rotor 1 amplitude in *x* direction

In Figure 11, the amplitude of *x* direction has been multiplied by "-1" so that its variation can be better shown. Figures 10 and 11 show that increasing of the misalignment angle increases the amplitude of rotor 1 slightly in *z* direction while, it increases significantly in *x* direction. The reason is due to the selected value of Z_o/ε. the three dimensional diagram of amplitude in *z* direction for Z_o/ε=.05 is illustrated in Figure 12, and shows the same response to misalignment as that in *x* direction.

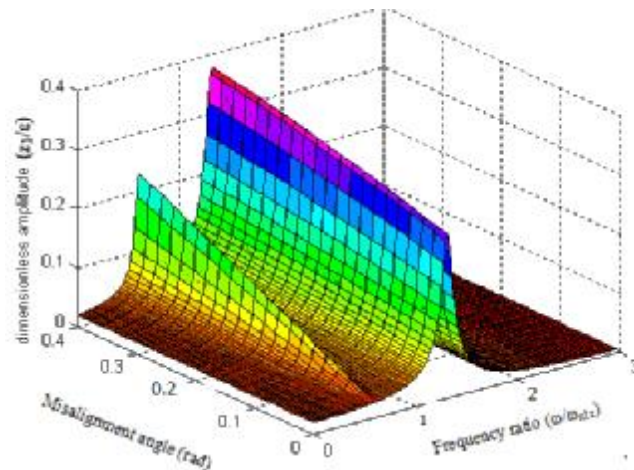**Figure 10.** Three dimensional diagram of rotor 1 amplitude in *z* direction

Figure 12. Three dimensional diagram of rotor 1 amplitude in *z* direction for Z_o/ε=0.05

Rotors 1 and 3 have the same positions in the model (Figure 2) and hence their amplitude response would be similar. So, the amplitude responses of rotor 3 have been studied in details.

9. SUMMARY AND CONCLUSIONS

In this study, a model for the lateral vibrations of three rotors subjected to the pure angular misalignment has been developed. The degrees of freedom of the system are the lateral deflections and the rigid-body rotation. The equations of motion of the system are obtained using the Lagrange equations through successive partial differentiations of the kinetic and potential energies. The equations of motion are coupled in the stiffness matrix and the force vector as a result of the presence of misalignment. The frequency spectrums revealed harmonics at the vibration amplitudes.

It is interesting that the foregoing study did not provide any evidence of the presence of harmonics of (1x) and (2x) which observed in the field of misaligned rotating systems.

Three dimensional diagrams of Figures 10 to 12, revealed that the angular misalignment would increase the axial and lateral vibration amplitudes.

It is suggested that the nonlinearities of the bearing, rotation of rotor 2 around the y axis and the dynamic response of the parallel misalignment be studied. Work is currently underway to model the influence of these parameters on the vibration response of the system.

Nomenclature

E — Modulus of elasticity

I_2 — Area moment of inertia of rotor 2

$\bar{I}_p$ — Polar mass moment of inertia of rotor p, $p = 1, 2, 3$

K_{eq} — Roller bearing's stiffness

k_2 — Bending stiffness of rotor 2

k_{cp} — Connection stiffness in direction of p, $p = x, y, z$

k_{bmp} — Stiffness of the Motor side bearing in direction of p, $p = x, y, z$

k_{bgp} — Stiffness of the Gearbox side bearing in direction of p, $p = x, y, z$

l_2 — Length of rotor 2

L — Length of the rollers of roller bearing

N — Number of rollers of the roller bearings

P — Load that is inserted on the roller bearing

r_{c21} — Displacement vector of end of rotor 2 in direction of rotor 1 unit vectors

r_{c23} — Displacement vector of end of rotor 2 in direction of rotor 3 unit vectors

T_p — Kinetic energy of rotor p, $p = 1, 2, 3$

U — Total potential energy

U_2 — Bending potential energy of rotor 2

U_{bm} — Potential energy of the motor side bearing

U_{bg} — Potential energy of the gearbox side bearing

U_{c21} — Potential energy of the connection of the rotors 1 and 2

U_{c23} — Potential energy of the connection of the rotors 2 and 3

x_p, y_p, z_p — Displacement of rotor p in directions of x, y and z $p = 1, 2, 3$

x_o, y_o, z_o — Rotor 2 end displacements in direction of x, y and z

x_{r2}, y_{r2} — Relative displacements of the center of mass and the end of rotor 2

Greek symbols

ε — Eccentricity magnitude of rotor 2

γ — Angular misalignment magnitude

α — Orientation change of the spacer due to the angular misalignment

φ — Phase delay of the deflection relative to the eccentricity of rotor 2

β_p — Rotation angle of rotor p $p = 1, 2, 3$

ζ_{ip} — Damping ratio of rotor p in direction of i, $p = 1, 2, 3$, $i = x, y, z$

ζ_2 — Damping ratio of the rotor 2

ω_{nip} — Natural frequency of rotor p in direction of i, $p = 1, 2, 3$, $i = x, y, z$

ω_{n2} — Natural frequency of rotor 2

10. REFERENCES

1.   Al-Hussain, K. M. and Redmond, I. "Dynamic response of two rotors connected by rigid mechanical coupling with parallel misalignment" *Journal of Sound and Vibration* 249 (3) (2002) 483–498.

2.   Lorenzen. H. E.A. Niedermann, W. Wattinger, "Solid couplings with flexible intermediate shafts for high speed turbo compressor trains" *Proceedings of the 18th turbo machinery Symposium, Dallas, TX, U.S.A.* 101-110.

3.   Sekhar, A. S. and Prabhu, B. S. Effects of coupling misalignment on vibrations of rotating machinery. *Journal of Sound and vibration.* (1995) 185, 655-671.

4.   Xu, M. and Marangoni, R. D. Vibration analysis of a motor-flexible coupling-rotor system subjected to misalignment and unbalance. Part I: theoretical model analysis. *Journal of Sound and vibration.* (1994) 176, 663-679.

5.   Prabhu, B. S. An experimental investigation on the misalignment effects in journal bearings. *STLE Tribology Transaction.* 1997*s* 40, 235-242.

6.   Simon, G. Prediction of vibration of large turbo-machinery on elastic foundation due to unbalance and coupling misalignment. *Proceedings of the Institution of Mechanical Engineers*, (1992), Vol. 206, 299.

7.   Al-Hussain, K. M. Dynamic stability of two rigid rotors connected by a flexible coupling with angular misalignment. *Journal of Sound and Vibration*, 266 (2003) 217–234

8.   Parshad, H. Relative comparison of stiffness and damping properties double ducker high precision and conventional rolling element bearings. *tribology international,* volume 35, (2002)

9.   Zhenwei Yuan, et al. External and internal coupling effects of rotor's bending and torsional vibrations under unbalances *Journal of Sound and Vibration,* 299, (2007), 339–347

10.   Thomson, W, T. and Dahleh, M, D. Theory of vibration with applications. John Villy and sons,